AN INVESTIGATION OF REAL-TIME DYNAMIC DATA DRIVEN
TRANSPORTATION SIMULATION

Michael P. Hunter

School of Civil and Environmental Eng.
Georgia Institute of Technology
Atlanta, GA 30332, U.S.A.

Richard M. Fujimoto

College of Computing
Georgia Institute of Technology
Atlanta, GA 30332, U.S.A.

Wonho Suh
Hoe Kyoung Kim

School of Civil and Environmental Eng.
Georgia Institute of Technology
Atlanta, GA 30332, U.S.A.

ABSTRACT

Widespread deployment of sensors in roadways and vehicles is creating new challenges in effectively exploiting the wealth of real-time transportation system data. However, the precision of the real-time data varies depending on the level of data aggregation. For example, minute-by-minute data are more precise than hourly average data. This paper explores the ability to create an accurate estimate of the evolving state of transportation systems using real-time roadway data aggregated at various update intervals. It is found that simulation based on inflow data aggregated over a short time interval is capable of providing a superior representation of the real world over longer aggregate intervals. However, the perceived improvements are minimal under congested conditions and most pronounced under un-congested conditions. In addition, outflow constraints should be considered during congested flow periods, otherwise significant deviation from the real world performance may arise.

1 INTRODUCTION

Recently, in an effort to boost research on real-time data application/simulation, the National Science Foundation (NSF) implemented research support aimed at Dynamic Data Driven Application Systems (DDDAS). The NSF definition of DDDAS is as follows:

DDDAS is a paradigm where application/simulations and measurements become a symbiotic feedback control system. DDDAS entails the ability to dynamically incorporate additional data into an executing application, and in reverse, the ability of an application to dynamically steer the measurement process (NSF 2005).

Traffic management is an example of an area likely to benefit from DDDAS. For example, at a local level, intersection based simulations may receive information from individual sensors, perform corridor simulations, and optimize signal control parameters to minimize delay. In an area-wide implementation, as illustrated in Figure 1, a number of local area simulations (potentially residing on individual vehicles, intersection controllers, or dedicated base stations) may be operating concurrently within the vehicle and roadside infrastructure to accurately determine the current state of the system and provide predictions of potential future states. This information may be utilized to provide desirable routes to travelers, optimize traffic signal timings, or to manage local area and system wide vehicle's ingress and egress.

A key to the successful implementation of such dynamic data driven transportation simulations is the ability to convert real-time field data into useful information in order to predict traffic conditions more accurately and efficiently. As sensors on the roadway continue to proliferate, the transportation-related data will expand by orders of magnitude. However, communications and computer processing are limited. Therefore, it should be determined which data are most effective and at what resolutions the data should be collected.

This paper investigates an example use of transportation field data, particularly traffic flows, in a dynamic data driven simulation. A simulation of the Georgia Institute of Technology (Georgia Tech) network is utilized to represent the real world, with flow data from the Georgia Tech model provided to a smaller simulation of two intersections within the network. The "real-world" flow data (i.e. flow data measured from the large scale Georgia Tech model) is aggregated in different intervals and used to dynamically drive the two intersection model. The desire of this study is to explore how well the small scale simulation model is able to reflect the real world scenario when fed data at different aggregation levels. This paper explores congested (referred to as peak hour) and un-congested (referred to as non-peak hour) traffic demand at data five different aggregation time intervals: 1 sec., 10 sec., 30 sec., 60 sec., and 300 sec.
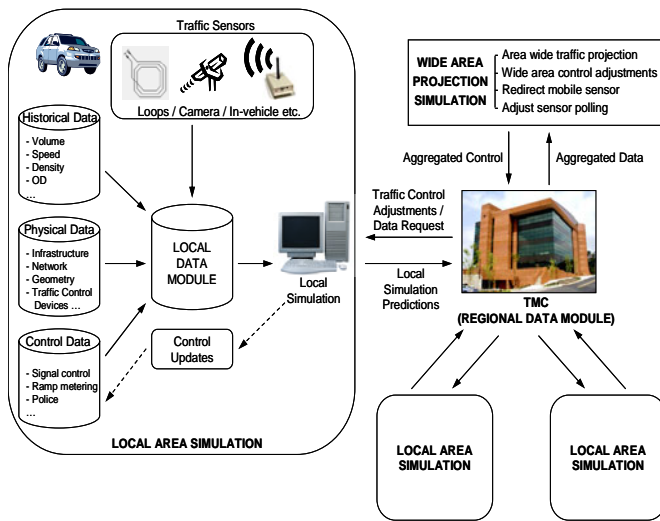
Figure 1: Dynamic Data Driven Traffic Management

2 EXPERIMENTAL DESIGN

This section introduces the microscopic transportation simulation VISSIM, defines the study area, and discusses the simulation approach, vehicle generations, outflow constraints and scenarios.

2.1 VISSIM

Both the two intersection simulation and real world Georgia Tech network simulation are modeled using the VISSIM microscopic surface transportation simulator. VISSIM is a discrete, stochastic and time step based microscopic simulation model developed to model urban traffic and public transit operations. The model is a useful tool for the evaluation of various alternatives based on transportation engineering and planning measures of effectiveness *(PTV 2005)*. Individual vehicles are modeled in VISSIM using a psycho-physical driver behavior model developed by Wiedemann *(PTV 2005)*. The underlying concept of the model is the assumption that a driver can be in one of four driving modes: free driving, approaching, following, or braking. The model was originally developed at the University of Karlsruhe, Germany during the early 1970s. VISSIM version 4.10, the latest release of the software at the time of this analysis, is used in this paper.

2.2 VISSIM Traffic Assignment: Trip Chain

Traffic assignment using the trip chain feature in VISSIM allows the traffic analyst to specify the traffic demand. Trip chains are assigned in an FKT file (Figure 2) and provide the simulation with detailed individual vehicle travel plans, including vehicle number, vehicle type, origin zone number, departure time, destination zone number, activity

number, and minimum stay time. In this paper, each vehicle is assigned a trip chain specifying the vehicle's departure time (time the vehicle wishes to enter the simulation) and destination.

Figure 2: VISSIM Trip Chain File

2.3 Study Area

Figures 3 illustrates the VISSIM networks utilized for this study. The large network (solid line), which represents the real world, incorporates the eastern portion of the Georgia Tech campus. It covers the area from Atlantic Drive on the east to West Peachtree Street on the west, with east-west connectivity provided via Fifth Street. The large network contains 14 intersections. The local network (dashed line) which receives data from the large model, consists of two signalized intersections along Fifth St. (Techwood Dr. and Spring St.), where Fifth St. crosses the I-75/I-85 downtown connector. This section of Fifth St. was chosen as it represents a critical connection and potential bottleneck between the east and west sides of campus.

Figure 3: Study Area

Geometric and traffic data for the models were collected as part of a field survey. Field data included signal data (cycle length, phase, phase sequence, and offsets), geometric layout (number of lanes, turn bay presence, link length, etc.), and directional traffic volume. However, for this study notional volumes were generated to represent congested and un-congested conditions in the area of the

local simulation. For the network, the vehicle fleet is assumed to be 100% autos, each with an desired speed of 30 mph. The model was calibrated to ensure traffic operations were realistic and representative. Performance measures for each local simulation presented in this paper are based on six replicate runs.

2.4 Simulation Approach

Figure 4 presents the VISSIM link illustration of the Georgia Tech simulation model, that is, the large network simulation (LNS). Enclosed within the dashed box are the intersections included within the local simulation (LS). The simulation model executions in this paper assume that vehicle inflow data are able to be collected and aggregated at Point A and Point D with the aid of advanced sensor technologies, such as loop detectors, video detectors, or in-vehicle sensors. The aggregate data are then transmitted to the local simulation, providing a dynamic (updating every aggregation interval) data driven arrival rate. The performance of the local simulation is tested using five different update time intervals: 1 sec., 10 sec., 30 sec., 60 sec., and 300 sec.
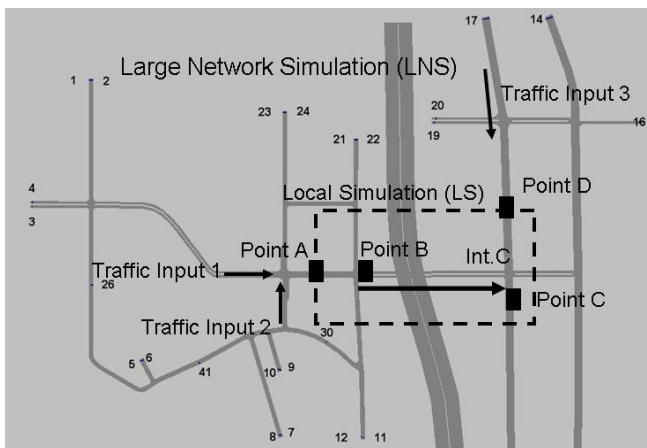

Figure 4: Georgia Tech Large Network Simulation and Local Simulation - VISSIM Link Diagram

2.5 Vehicle Generations

At the beginning of the large network simulation run, the system is empty. Vehicles are generated at the entry nodes of the network, based on the selected input volumes and an assumed headway distribution. This initial research effort utilized a negative exponential distribution (May 1990) to simulate the arrival of vehicles at the large network entry nodes. Thus, vehicles are generated with time headways according to:

$$h = H \times [-\ln(1 - R)].$$

where:

H = mean headway for the time period (sec.)
h = headway separating each generated vehicle (sec.)
R = random number (0 to 1.0)

The arrival rate for the local simulation at Point A and Point D is based on the aggregate arrivals measured on the large simulation. The local simulation vehicle generation during an aggregation interval follows a uniform distribution for the given arrival rate. Thus, over the analysis period, the total number of vehicles generated at Point A and Point D of the large network simulation and the local simulations are identical. This allows for a direct comparison (or pairing) of an individual vehicle's trip characteristics, i.e. arrival time at an intersection, delay, travel time, etc., in the large network and its simulated trip characteristics in the local network.
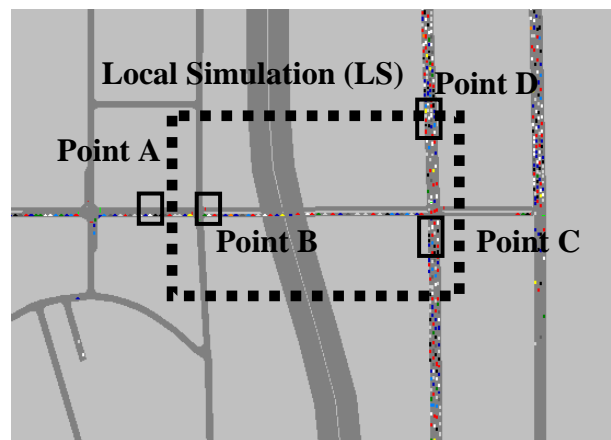

Figure 5: Simulation Snapshot at Peak Hour

2.6 Traffic Demands and Scenarios

As stated previously, the objective of this analysis is to explore how well the local simulation reflects the large network simulation based on the different aggregation intervals. For this study it is also desired to determine the impact on the local simulation performance when the real world situation is deemed either congested or un-congested. In order to model these traffic conditions, representative travel demands and arrival patterns were generated.

Four un-congested scenarios and four congested scenarios were modeled. In the large simulation un-congested scenarios 1 and 2 and congested scenarios 5 and 6, traffic is generated such that the local simulation will receive vehicles from traffic streams at traffic inputs 1, 2, and 3, and in the remaining scenarios from traffic inputs 1 and 3 (Figure 4). Local simulation arrival streams are generated at the intersecting points (dashed box in Figure 5) with the large network simulation, at the given aggregation interval. Each model is run for a total of 120 minutes. The un-

congested and congested scenarios modeled are given in Table 1 and Table 2, respectively.

Table 1: Non-Peak Traffic Input (Un-Congested)

Scenario No	Traffic Input No.	Time (min)	Input (vphpln)	Outflow Constraint
1	1	0-120	240	No
	2	0-120	240	
	3	0-120	500	
2	1	0-120	240	Yes
	2	0-120	240	
	3	0-120	500	
3	1	0-120	480	No
	2	0-120	0	
	3	0-120	500	
4	1	0-120	480	Yes
	2	0-120	0	
	3	0-120	500	

Table 2: Peak Traffic Input (Congested)

Scenario No	Traffic Input No.	Time (min)	Input (vphpln)	Outflow Constraint
5	1	0-30	240	No
	1	30-90	360	
	1	90-120	240	
	2	0-30	240	
	2	30-90	360	
	2	90-120	240	
	3	0-30	500	
	3	30-90	750	
	3	90-120	500	
6	1	0-30	240	Yes
	1	30-90	360	
	1	90-120	240	
	2	0-30	240	
	2	30-90	360	
	2	90-120	240	
	3	0-30	500	
	3	30-90	750	
	3	90-120	500	
7	1	0-30	480	No
	1	30-90	720	
	1	90-120	480	
	2	0-30	0	
	2	30-90	0	
	2	90-120	0	
	3	0-30	500	
	3	30-90	750	
	3	90-120	500	
8	1	0-30	480	Yes
	1	30-90	720	
	1	90-120	480	
	2	0-30	0	
	2	30-90	0	
	2	90-120	0	
	3	0-30	500	
	3	30-90	750	
	3	90-120	500	

2.7 Outflow Constraint

As seen in Tables 1 and 2, for several of the scenarios an outflow constraint is referenced. This refers to an outflow constraint placed at Point C (Figure 5) in the local simulation. This constraint meters the outflow from the local simulation model, allowing for a potentially more accurate reflection of the large simulation network. The need for outflow metering is particularly critical where traffic constraints outside the boundaries of the local simulation may result in a spillback of congestion into the region being modeled. Figure 5 provides a snapshot of such a scenario, where congestion on Fifth Street and Spring Street is a result of a traffic bottleneck outside the bounds of the local simulation (dashed box). For the experiments in this effort, the local simulation outflow constraint is provided by utilizing the VISSIM reduced speed zone module. This module forces vehicles within the zone to reduce their speed. By reducing the vehicle speeds at Point C to the speeds being experienced in the large simulation, it becomes possible to better reflect the large network operations. Currently, vehicle speed data at Point C are collected and aggregated in ten minutes intervals and then transmitted to the dynamic data driven local simulation.

3 PERFORMANCE MEASURE COMPARISONS

To examine how well the data driven application (local simulation) reflects the real world transportation system (large simulation) data collection points are placed at the beginning and end of the link connecting Point B and Intersection C. For each vehicle, the time the vehicle arrives at Point B and the delay on the link (where delay is the difference between actual and desired travel time) between Point B and Intersection C (i.e. the key link over the freeway) is measured in both the large and local simulation. The primary consideration in this analysis is the difference in the vehicle's modeled arrival and delay values. The differences are computed for each vehicle pair (i.e. the vehicle in the large simulation model and the simulation of that vehicle in the local model) and then aggregated in thirty minute intervals, where average and root mean square error (RMSE) values are calculated for each thirty minute interval.

The results for the un-congested (non-peak) conditions are presented first, followed by the congested (peak) conditions.

3.1 Non-peak Conditions

Table 3 presents un-congested condition arrival time differences at Point B for the five local simulation inflow aggregation intervals during the 60 to 90 minute time interval. Figure 6 provides an example of large vs. local simulation individual vehicle arrival time differences. It is readily seen that the local network with one second aggregation intervals provides the highest degree of agreement with the large simulation, with an 0.0 sec. to 0.2 sec. average arrival time difference and 1.0 sec. to 2.0 sec. RMSE. The 1-second scenario does not provide an exact replication of the large model arrival pattern as vehicle generation in the local model is limited to the nearest second. For ex-

ample, a vehicle that arrives at Point A at 10.4 sec. in the large network is generated at time 10.0 sec. in the local network, leaving 0.4 sec. difference with the large network simulation. Also, the VISSIM trip chain feature utilized to generate the traffic in the local maintains a strict minimum headway between vehicles during vehicle generation. Thus, a tight platoon in the large simulation model might be slightly dispersed in the local simulation.

For the remaining aggregation scenarios, the average arrival time differences stay relatively low, ranging from -9.7 sec. to 2.2 sec. The scenario 3 and 4, 300 sec. aggregation interval simulation even achieves an average arrival time difference of 0.0 sec. However, there exists a clear trend of increasing RMSE values as the aggregation interval increases. Thus, even though the average arrival time values may be similar between the large and local simulations, there is a clear sense of increasing variation in actual arrival patterns between the two simulations and potentially significant arrival time differences between individual vehicles. Figure 6 presents an example plot of the vehicle arrivals over a 300 second time interval for all aggregation intervals. From these results it can be seen that the average arrival time difference alone is likely not a good indicator of the ability of a data driven simulation to reflect the real world operations. Measures of variation such as RMSE should also be considered.

It is also noted from Table 3 that the performance difference is partially dependent upon the arrival pattern. For example, the average arrival time differences for the 60 sec. and 300 sec. aggregation intervals under scenarios 1 and 2, (-4.6 sec. and -9.7 sec., respectively) are significantly less than those under scenarios 3 and 4 (2.2 sec. and 0.0 sec., respectively). In addition, the RMSE values are greater in scenarios 1 and 2. These results imply that the vehicle arrival pattern will impact the quality of a dynamic data driven simulation. In these scenarios, there is some evidence that as the likelihood of vehicle platooning is minimized and the quality of coordination between signals deteriorates (e.g. the more random the vehicle arrivals) the local dynamically driven simulation will more closely reflect the large simulation. Future efforts will attempt to support and quantify the impact of vehicle arrival pattern on the data driven simulation.

The calculated average vehicle delay difference and RMSE on the link from Point B to Intersection C are shown in Table 4 and Figure 7. The delay comparisons reflect characteristics similar to the arrival time comparisons. Minor differences in average delays are seen as the aggregation interval increases, however the RMSE clearly increases with the aggregation interval. Once again the vehicle arrival pattern is also shown to impact the how well the local simulation is able to reflect the large simulation.

Table 3: Arrival Time Comparison (Non-Peak, 60-90min.)

Scenario / Agg. Interval		1sec	10sec	30sec	60sec	300sec
1	AATD*	0.2	0.3	-1.2	-4.6	-9.7
	RMSE	2.0	3.5	10.3	15.6	26.4
2	AATD*	0.2	0.3	-1.2	-4.6	-9.7
	RMSE	2.0	3.5	10.3	15.6	26.4
3	AATD*	0.0	0.0	1.7	2.2	0.0
	RMSE	1.0	1.8	10.3	13.0	17.1
4	AATD*	0.0	0.0	1.7	2.2	0.0
	RMSE	1.0	1.8	10.3	13.0	17.1

AADT* - Average Arrival Time Difference (LNS – LS)

Table 4: Delay Comparison (Non-peak, 60-90min.)

Scenario / Agg. Interval		1sec	10sec	30sec	60sec	300sec
1	ADD*	0.0	-0.9	-0.6	-0.5	0.6
	RMSE	5.8	6.9	10.6	14.5	20.0
2	ADD*	-0.1	-0.9	-0.7	-0.5	0.6
	RMSE	6.0	7.1	10.6	14.5	20.0
3	ADD*	-0.2	-0.5	-0.7	-0.1	-0.3
	RMSE	6.2	5.9	11.2	13.4	15.9
4	ADD*	-0.3	-0.6	-0.8	-0.1	-0.3
	RMSE	6.1	6.4	11.2	13.4	15.9

ADD* - Average Delay Difference (LNS – LS)

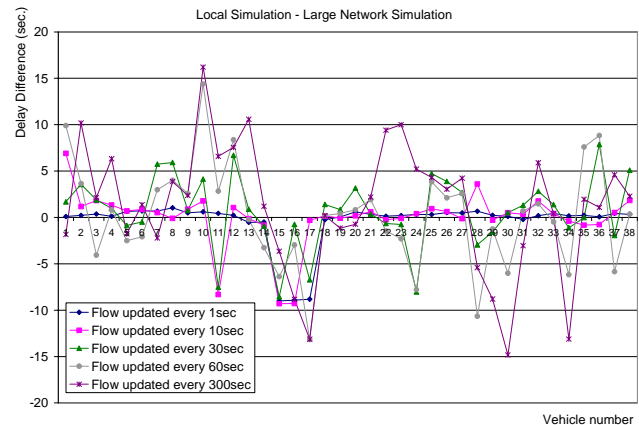Figure 6: Arrival Time (Non-Peak, 4000 sec.-4300sec.)

Figure 7: Delay Difference (Non-Peak, 4000 sec.-4300sec.)

Figure 7 displays the delay difference for a series of 38 vehicles, with the delay difference being the delay experienced by the vehicle in the large simulation minus the same vehicle's simulated delay in the local simulation. The minimal variation is clearly seen at the lower aggregation levels with the large variations at the longer aggregation intervals.

Finally, for the un-congested conditions little difference is seen between those scenarios with and without the outflow constraint. This is a reasonable result as in un-congested conditions, vehicles are able to maintain their desired speed on Spring St., the location of the modeled outflow constraint. Thus, the speed constraint is consistently near the free flow speed, offering minimal hindrance to vehicles exiting the local network.

3.2 Peak Condition

In the peak congestion scenarios, the challenging, and more likely, case of congested conditions extending beyond the bounds of the local simulation is considered. Comparison of the arrival time at Point B for the congested scenario conditions is presented in Table 5. Unlike the un-congested conditions the average arrival time is considerably different for a vehicle in the large simulation than that simulated in the local model. Arrival time differences range from -10.8 seconds to 58.5 seconds. There is also not a clear trend of the local simulation providing an improved reflection of the large simulation under the smaller aggregation intervals. Significant differences are also seen in the delay comparison between the large and local model, again with no clear advantage demonstrated between the different aggregation intervals in either the average values or the RMSE. This result implies that the impact of congestion on the ability of a data driven local simulation to reflect a portion of a real world network can dominate the impact of a selected aggregation interval. The accuracy of the initial vehicle generation pattern does not help the local network effectively reflect the large network, as any benefit of more accurate vehicle entrance times are lost in the inaccuracies of the congestion model.

Table 5: Arrival Time Comparison (Peak, 60-90min.)

Scenario / Agg. Interval		1sec	10sec	30sec	60sec	300sec
5	AATD*	54.4	55.2	55.0	54.1	53.1
	RMSE	58.1	58.7	59.0	59.0	58.3
6	AATD*	30.3	16.6	13.9	20.4	-10.8
	RMSE	43.5	51.5	53.6	40.7	67.8
7	AATD*	56.3	57.0	56.8	55.9	58.8
	RMSE	60.1	60.7	60.8	61.1	63.4
8	AATD*	21.5	28.4	14.1	8.7	37.0
	RMSE	61.7	54.5	53.0	54.5	52.5

AATD* - Average Arrival Time Difference (LNS – LS)

The impact of traffic arrival patterns is also overwhelmed by the congestion. For example, the scenario 5 and 7 average arrival time differences, delay differences, and RMSE's are similar for all aggregation intervals, even though the traffic arrival patterns are different. These results imply that different arrival patterns do not have a significant influence on the arrival time and delay under congested conditions.

Table 6: Delay Comparison (Peak, 60-90min.)

Scenario / Agg. Interval		1sec	10sec	30sec	60sec	300sec
5	ADD*	205.9	205.2	207.0	207.1	207.7
	RMSE	209.8	209.1	211.0	211.2	211.8
6	ADD*	37.0	26.5	30.4	22.7	24.6
	RMSE	60.3	64.4	62.3	53.0	73.5
7	ADD*	217.8	217.0	218.2	218.8	219.1
	RMSE	221.0	220.2	221.5	222.4	222.7
8	ADD*	23.5	44.1	29.8	24.5	24.9
	RMSE	53.3	69.2	56.4	61.3	53.7

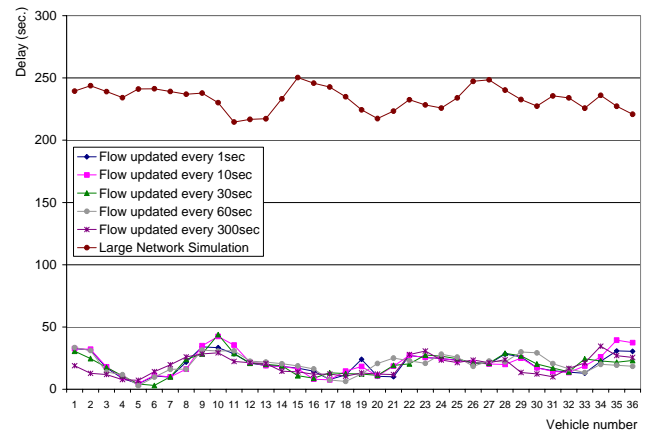ADD* - Average Delay Difference (LNS – LS)

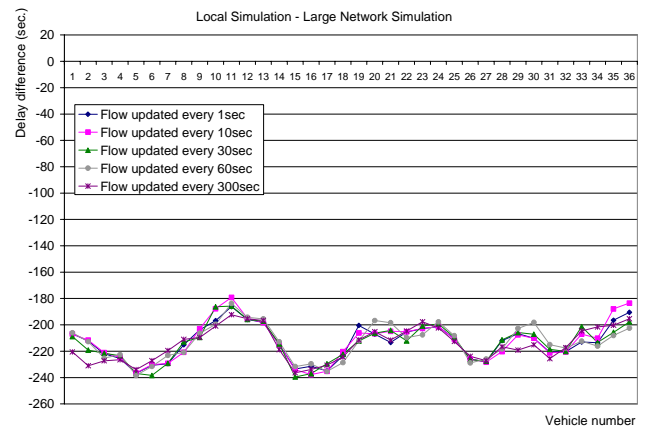Figure 8: Delay (Peak Without Outflow Constraint, 4000 sec.-4300sec.)

Figure 9: Delay difference (Peak Without Outflow Constraint, 4000 sec.-4300sec.)

However, the use of the outflow constraints clearly impacts the quality of the local simulation's reflection of the large simulation. The results with the outflow constraint at Point C (scenarios 6 and 8) show significant improvements over the scenarios without the outflow constraint (scenarios 5 and 7). For example, Figures 8 and 9 illustrate the scenario 6 (no outflow constraint) delay and delay difference experienced by each vehicle for the time period 4000 sec. to 4300 sec. It is readily seen that the local simulation provides a very poor reflection of the large simulation. The failure of the local simulation to capture the operation of the large simulation results from the severe congestion on Spring St. due to a bottleneck that occurs outside the area modeled by the local simulation. The congestion on Spring St. spills back into the area modeled by the local simulation, resulting in severely degraded performance at the intersection of Fifth St. and Spring St. With the congestion spillback from the downstream bottleneck, the Fifth St. intersection is unable to process the vehicle capacity that is implied by the given signal control and intersection geometry. Figure 10 shows a snapshot of the perceived congestion at the intersection of Fifth St. and Spring St. under the local simulation (without and with outflow constraint). In both instances the same traffic demand arrives at the Fifth St. intersection. As seen in Table 6 the delays measured on the local simulation without an outflow constraint are significantly less than that actually experienced in the large scenario.
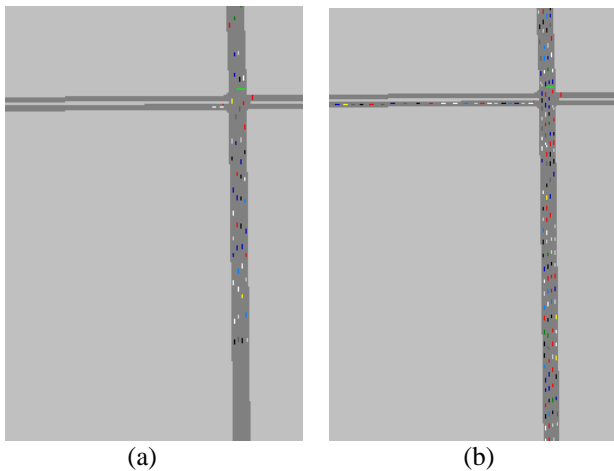

(a)   (b)

Figure 10: Simulation Snapshot (Peak at 90min.) (a) Without & (b) With Outflow Constraint

Clearly, the impact of a bottleneck downstream of the local simulation can have a significant impact on operations within the area modeled by the local simulation. Thus, it is necessary to capture the repercussions of such bottlenecks in the local simulation. Scenarios 5 and 7 capture the downstream bottleneck by enforcing an outflow constraint in which the average speed of vehicles on local simulation exit link (i.e. Point C - Spring St. south of Fifth) are adjusted to match the speeds on the large simulation, essentially constraining the outflow from the local simulation to be similar to that of the large simulation. As a result, the delay model on the local simulation provides a significantly superior reflection of the large simulation (Figures 11 and 12). However, even with the outflow constraint, differences between the local and large model exist at all aggregation levels. Future research efforts will be centered on improving the performance of the dynamically data driven local simulation model under congested conditions.
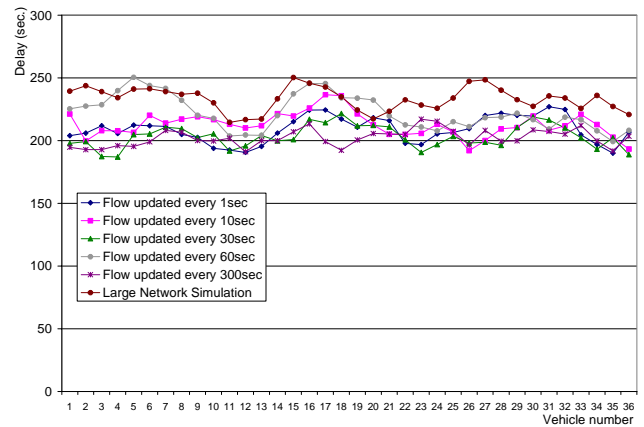

Figure 11: Delay (Peak With Outflow Constraint, 4000 sec.-4300sec.)
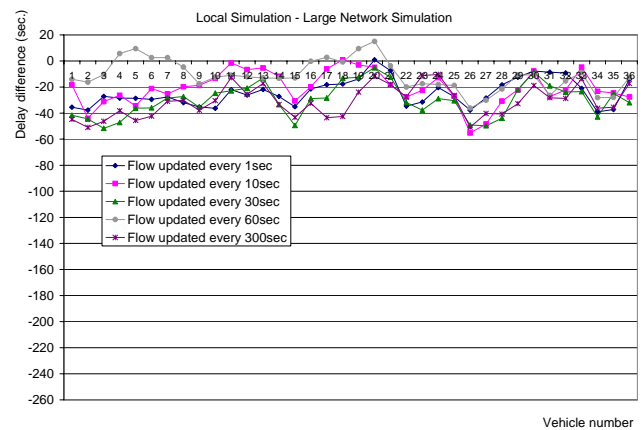

Figure 12: Delay Difference (Peak With Outflow Constraint, 4000 sec.-4300sec.)

4   CONCLUSIONS

This paper began the exploration of the ability to create an accurate estimate of the evolving state of a local transportation system using real-time roadway data aggregated at various update intervals. In the modeled "real world" traffic, the VISSIM trip chain feature is used as it has the advantage of allowing for the specification of individual vehicle departure times and paths. An assumption

of this effort is that vehicle flow data are able to be collected, aggregated, and transmitted to a dynamic data driven local simulation at varying update intervals..

For the un-congested conditions, there existed minor differences in the average value of the considered performance metrics (arrival time and delay) and the performance metric difference values for the tested scenarios. However, there was a clear trend of increasing RMSE's as the aggregation interval increased. Varying the upstream origin of the arrival streams also tended to influence the RMSE values more than the average values. From these results it can be seen that under un-congested conditions, the average of performance metrics alone are likely not good indicators of the ability of a data driven simulation to reflect real world operations. Measures of variation such as RMSE should also be considered.

Unlike the un-congested conditions, the average values of the performance metrics in congested conditions were considerably different for the large real world simulation than the local simulation. The RMSE values also were significantly greater that those in the un-congested scenarios. There is also not a clear trend of the local simulation providing an improved reflection of the large simulation when given the smaller aggregation intervals. For the tested scenarios, the impact of congestion dominated the impact of a selected aggregation interval and upstream arrival pattern. The use of outflow constraints significantly improved the local model performance. These constraints helped capture the impact on the local simulation of congestion that occurs outside the local model boundaries. Where the boundaries of the congested region fall outside of the local simulation it becomes readily apparent that both the inflow and outflow parameters of the simulation must be dynamically driven to achieve a reasonable reflection of the real world conditions.

As sensor technologies have advanced, the amount of available real-time field data has increased dramatically. The quantity of available real-time data is expected to continue to climb at an ever-increasing rate. This tidal wave of real-time data opens the floodgates to potential data driven transportation applications. This effort has begun to examine some of the innumerable potential uses of this data.

REFERENCES

May, A. D., *Traffic Flow Fundamentals*, Prentice-Hall, 1990.

National Science Foundation (NSF). 2005. *DDDAS: Dynamic Data Driven Applications Systems*. Available online via <http://www.nsf.gov/funding/pgm_summ.jsp?pims_id=13511> [accessed May 15, 2006].

PTV, *VISSIM User Manual 4.10*. Karlsruhe, PTV Planung Transport Verkehr AG, 2005.

AUTHOR BIOGRAPHIES

MICHAEL HUNTER is an assistant professor in the School of Civil and Environmental Department at the Georgia Institute of Technology. His primary areas of interest are traffic safety, operational performance and control, and simulation. He earned his Ph.D. at the University of Texas at Austin in August 2003. His e-mail address is <michael.hunter@ce.gatech.edu>.

RICHARD FUJIMOTO is a professor in the College of Computing at the Georgia Institute of Technology. He received his Ph.D. and M.S. degrees from the University of California (Berkeley) in 1980 and 1983. Among his current activities he is the technical lead concerning time management issues for the DoD High Level Architecture (HLA) effort, is an area editor for ACM Transactions on Modeling and Computer Simulation, and has also been chair of the steering committee for the Workshop on Parallel and Distributed Simulation, (PADS) since 1990. His email address is <fujimoto@cc.gatech.edu>.

WONHO SUH is a Ph.D. student at the Georgia Institute of Technology. Prior to joining Georgia Tech, he worked as a research engineer for five years at Yooshin Corporation in South Korea. He holds an M.S. in Civil Engineering from Seoul National University (2000). His current research interest is in microscopic traffic simulation. His e-mail address is <wonho.suh@gatech.edu>.

HOE KYOUNG KIM is a Ph.D. student at the Georgia Institute of Technology. His primary research interest is adaptive traffic signal control system, arterial performance evaluation and microscopic simulation. He obtained his M.S. in the Department of Civil Engineering at Texas A&M University (2002). His e-mail address is <gtg199j@mail.gatech.edu>.